Accepted Manuscript

Inhibition of pyruvate kinase M2 by reactive oxygen species contributes to the development of pulmonary arterial hypertension

Dongqing Guo, Junzhong Gu, Hui Jiang, Asif Ahmed, Zhiren Zhang, Yuchun Gu

Please cite this article as: Guo Dongqing, Gu Junzhong, Jiang Hui, Ahmed Asif, Zhang Zhiren, Gu Yuchun, Inhibition of pyruvate kinase M2 by reactive oxygen species contributes to the development of pulmonary arterial hypertension, *Journal of Molecular and Cellular Cardiology* (2016), doi: 10.1016/j.yjmcc.2016.01.009

This is a PDF file of an unedited manuscript that has been accepted for publication. As a service to our customers we are providing this early version of the manuscript. The manuscript will undergo copyediting, typesetting, and review of the resulting proof before it is published in its final form. Please note that during the production process errors may be discovered which could affect the content, and all legal disclaimers that apply to the journal pertain.

Inhibition of pyruvate kinase M2 by reactive oxygen species contributes to the development of pulmonary arterial hypertension

Dongqing Guo[1], Junzhong Gu[1], Hui Jiang[2], Asif Ahmed[3], Zhiren Zhang[4] and Yuchun Gu[1,*]

[1] Molecular Pharmacology Laboratory, Institute of Molecular Medicine, Peking University, Beijing, China, 100871.

[2] Beijing Key Laboratory of Reproductive Endocrinology and Assisted Reproduction, Department of Urology, Peking University Third Hospital, Beijing, China, 100191.

[3] Aston Medical School, Aston University, Birmingham, U.K., B4 7ET.

[4] Department of Pharmacology, 2nd affiliated hospital of Harbin Medical University, Harbin, China, 150000.

A short title: PKM2 and pulmonary arterial hypertension

The number of words : 4777

Address for correspondence:
Yuchun Gu, MD, PhD
Chair in Molecular Pharmacology Laboratory,
Institute of Molecular Medicine (IMM), Peking University,
Room 216, Pacific Building, 52 Haidian Road
100871, Beijing, China
Tel: +86.10.8254.5679
Fax: +86.10.8257.5672
Email: ycgu@pku.edu.cn

Abstract

Aims: Pulmonary arterial hypertension[1] is a proliferative disorder associated with enhanced proliferation and suppressed apoptosis of pulmonary artery smooth muscle cells (PASMCs). Reactive oxygen species (ROS) is implicated in the development of PAH and regulates the vascular tone and functions. However, which cellular signaling mechanisms are triggered by ROS in PAH is still unknown. Hence, here we wished to characterize the signaling mechanisms triggered by ROS.

Methods and Results: By western blots, we showed that increased intracellular ROS caused inhibition of the glycolytic pyruvate kinase M2 (PKM2) activity through promoting the phosphorylation of PKM2. Monocrotaline (MCT)-induced rats developed severe PAH and right ventricular hypertrophy, with a significant increase in the P-PKM2 and decrease in pyruvate kinase activity which could be attenuated with the treatments of PKM2 activators, FBP and L-serine. The antioxidant NAC, apocynin and MnTBAP had the similar protective effects in the development of PAH. In vitro assays confirmed that inhibition of PKM2 activity could modulate the flux of glycolytic intermediates in support of cell proliferation through the increased pentose phosphate pathway (PPP). Increased ROS and decreased PKM2 activity also promoted the Cav1.2 expression and intracellular calcium.

Conclusion: Our data provide new evidence that PKM2 makes a critical regulatory contribution to the PAHs for the first time. Decreased pyruvate kinase M2 activity confers additional advantages to rat PASMCs by allowing them to sustain anti-oxidant responses and thereby support cell survival in PAH. It may become a novel treatment strategy in PAH by using of PKM2 activators.

Key words: ROS; PKM2; activators; pulmonary arterial hypertension.

1. Introduction

Pulmonary arterial hypertension[1] is a severe disease caused by increased pulmonary vascular resistance (PVR) and pulmonary pressure[2]. PAH is associated with structural alterations of the pulmonary vessels [3] and characterized by abnormal pulmonary vasoconstriction and structural remodeling of the small pulmonary arteries. Pulmonary artery smooth muscle cells (PASMCs) undergo suppressed apoptosis, enhanced proliferation and migration in the pathogenesis of PAH [4]. Such alterations can be caused and exaggerated by reactive oxygen species (ROS) [5].

ROS is critical to regulate vascular tone and functions [6]. In the lung, ROS is implicated in acute hypoxic vasoconstriction [7]. Nox-derived ROS is acutely activated in the pulmonary hypertension [8]. TGF-ß1 promotes HPASMC proliferation through a signaling pathway involving NOX4 induction [9]. Nox1, but not Nox4 is responsible for pathophysiological proliferation and migration of PASMCs in MCT-induced PAH via increased ROS [10]. However, mechanisms underlining cellular signal pathways triggered by ROS remain unclear.

The aerobic glycolysis involves conversion of glucose to lactate and the generation of ATP. Pyruvate kinase catalyzes the final step in glycolysis by transferring the phosphate from phosphoenolpyruvate (PEP) to ADP, thereby generating pyruvate and ATP [11]. The M2 isoform of pyruvate kinase (PKM2) is preferentially expressed in cancer [12] and is a central point of regulator in cancer metabolism [13]. PKM2 promotes the Warburg effect and tumorigenesis [14]. PKM2 is a PHD3-stimulated coactivator for hypoxia-inducible factor 1 in cancer [15]. Pyruvate kinase M2 promotes de novo serine synthesis to sustain mTORC1 activity and cancer cell proliferation [16]. PKM2 could also regulate ß-catenin transactivation, cell proliferation and tumorigenesis in the activation of EGFR [17]. What's more, PKM2 may confer an additional advantage to cancer cells by allowing them to withstand oxidative stress [18].

It is well recognized that PASMCs proceed fundamental similarities with cancer cells in the pathogenesis of PAH. It is therefore important to know how PKM2 contributes to the development of PAH. In this paper, we investigated the roles of PKM2 in the pathogenesis of PAH and found that PKM2 activity decreased in response to the increased oxidative stress in the PAH, suggesting that PKM2 plays a key role in the PAH and also PKM2 activators may serve a novel treatment strategy in PAH.

2. Methods

2.1 Animals

Animal experiments conformed to the Guide for the Institutional Animal Care and Use Committee (IACUC) and was approved by the Ethics Review Board for Animal Studies of Institute of Molecular Medicine (IMM), Peking University (Permit Number: IMM-GuYC-1). Adult male Sprague Dawley rats (250g) were purchased from Vital River (Beijing, China). Euthanasia was achieved by isoflurane inhalational anaesthesia (1.5%) and concurrent anaesthetic overdose as approved by the respective University IACUCs.

2.2 MCT treatment

Monocrotaline(MCT, Sigma) was administered as a single subcutaneous injection in a dose of 60 mg/kg body mass. Control rats received an equal volume of isotonic saline. Rats were sacrificed 28 days after MCT injection.

2.3 Measurement of right ventricle hypertrophy

Hearts were perfused with 0.9% saline and followed by constant-pressure infusion of saline for 30 min with needle inserted into the left ventricle and a small hole in the right atrium, resulting in removal of residual blood. Using a dissecting microscope, the atria/valves and extraneous vascular material were removed from the heart. The free wall of the RV was dissected from the left ventricle (LV) and septum (S) and both portions were quickly blotted dry. A weight ratio of RV/(LV+S) was calculated to determine right ventricular hypertrophy.

2.4 Isolation of pulmonary arterial smooth muscle cells

Rats were anesthetized and the lung vasculature was flushed via the pulmonary artery with 0.9% NaCl in order to remove the blood. PASMCs were derived from pulmonary arterioles using the method as previously described [19]. The purity and identity of PASMCs were confirmed using specific α-smooth muscle actin (α-SMA) antibodies, a protein marker for PASMCs.

2.5 Histology

The lung tissues were obtained from anesthetized rats, sliced into tissue blocks, and immersed in 4% paraformaldehyde for overnight fixation. Fixed tissues were then dehydrated, cleared, and embedded in paraffin wax. The tissues were cut into 5 μm thick sections and stained with hematoxylin and eosin (H&E). Results are expressed as the wall thickness. The sections were viewed with an Eclipse 600 Nikon microscope and photographed with a digital camera. Morphometric analysis was analyzed with Image J software.

2.6 Immunoblotting

Cells and lung tissues were lysed ice-cold RIPA lysis buffer (Solarbio) including PMSF and proteinase inhibitor cocktail (Roche). Samples were centrifuged for 15min at 12,000g at 4°C and the supernatants were harvested. About 60 ug of each protein sample were loaded and separated on 10% Bis-Tris Gel followed by transferring to 0.45 mm PVDF membrane. The membranes were then blocked with 5% non-fat dry milk, probed with appropriate primary antibodies, followed incubation by HRP-conjugated secondary antibodies at a dilution of 1: 5000. The following antibodies were used: rabbit anti-Phospho-PKM2 (Tyr105) (Cell Signaling, #3827), rabbit anti-PKM2 (Cell Signaling, #3198), mouse anti-ß-actin (Beijing TDY Biotech LTD, #M009), HRP-conjugated secondary mouse (Beijing TDY Biotech LTD, #E009) and rabbit antibodies (Beijing TDY Biotech LTD, #E011).

2.7 Quantitative RT-PCR

Total RNA was extracted from lung tissues and RPASMCs. mRNA was reverse transcribed using random primers and cDNA synthesis Kit (TransGen Biotech). The resulting cDNAs were mixed with the SYBR PCR master mix (TransGen Biotech) and run on the Step-One Plus Applied Biosystems Real-time PCR machine. One cycle of denaturing step (30 sec at 94°C) was applied, followed by 40 cycles of amplification (5 sec at 94°C and 30sec at 60°C), with fluorescence measured during the extension. 18s was as the house keeping gene to normalize the gene

expression. Calculations were performed by a comparative method ($2^{-\Delta\Delta Ct}$). Primers used in this study are listed below.

GPX1: F: 5'-GCTCACCCGCTCTTTACC-3'; R: 5'-AACACCGTCTGGACCTACC-3'

PHGDH: F: 5'-GGGGAGGAAATCGCAGTC-3'; R: 5'-TAGCGTTCACCAAGTTCACATC-3'

PSAT1: F: 5'-GGGGTGACGGTAGTGATT-3'; R: 5'-CATCCTGCTTCTATTCTGG-3'

PSPH: F: 5'-GTTGCCTTTCAAAGATGCG-3'; R: 5'-CGTGCTCCACAATACTCCTAA-3'

18s: F: 5'-CGAACGTCTGCCCTATCAACT-3'; R: 5'-CAGACTTGCCCTCCAATGGATCCTCGTT-3'.

2.8 PKM2 activity assay

PK activity was measured in an LDH-coupled enzymatic assay as described previously[20], either from cell extracts or rat serum.

2.9 Glucose, lactate and GSH/GSSG measurement

Cell media was collected from wells; spun down at high speed to remove any cell debris, deproteinized using TCA, pH was adjusted between 7.0-7.5 and then glucose uptake was analyzed using glucose assay kit (Sigma, #GAGO-20), according to manufacturer's protocols. Lactate was analysed using kit (BioAssay, ECLC-048) as per manufacturer's instructions. GSH/GSSH was analysed using kit (Beyotime, #S0055) according to manufacturer's protocols.

2.10 Proliferation assays

For determination of proliferation, MTT assay was used as reported previously. Briefly, RPASMCs were seeded at a density of 1,000 per well into 96-well cell culture plates and allowed them to adhere for 24h. After different treatments, 20 ml of MTT was added to each well for 3h incubation. Subsequently, cells were dissolved by 150 mL of DMSO, mixed and measured the absorbance (A) by Multiskan (Thermo) at 540nm. The relative proliferation rate was calculated by the absorbance ratio of the drug-treated group to the control group.

2.11 Measurements of Intracellular reactive oxygen species

Intracellular ROS was quantified by a laser confocal microscope using the fluorescent probe, 2′,7′-dichlorodihydrofluorescein diacetate (DCFH-DA). RPASMCs were incubated in phenol red-free media supplemented with 10 μM DCFH-DA in dark for 20 min at 37°C. They were then washed twice with PBS and immediately observed.

2.12 Calcium imaging

Calcium imaging was performed using Fura-8[TM] (AAT Bioquest) according to previous description. Fluorescence images of the cells were recorded and analyzed with a video image analysis system.

2.13 Statistical Analyses

The Student's t-test was used for the statistical analysis of all the independent experiments. Data are expressed as average ± SEM of at least three independent experiments. A p-value of <0.05 was considered statistically significant.

3. Results

3.1 Isolated pulmonary arterial smooth muscle cells were sensitive to the glycolysis inhibitor.

PASMCs are a major site of vascular remodeling underlying pulmonary hypertension [21]. To assess the key metabolic way of rat PASMCs (RPASMCs), RPASMCs were isolated from SD rats and stained for α-SMA (Data not shown). Then isolated RPASMCs were treated with different concentration of 2-DG and oligomycin. 2-DG is an inhibitor of glycolysis and oligomycin is the inhibitor of mitochondrial oxidative phosphorylation. As a result, 2-DG obviously inhibited intracellular ATP production of RPASMCs in a dosage-dependent manner, while oligomycin had no effect (Fig.1A). The data suggested that glycolysis was the dominant metabolic way for RPASMCs. The key enzymes involved in the glycolysis might function in the development of PAH.

3.2 P-PKM2 expression increased and pyruvate kinase activity decreased in the PAH.

MCT injection led to pulmonary hypertension with an increase in right ventricular systolic pressure (RVSP) and a right heart hypertrophy as depicted by the increment in the ratio of the right ventricle/(left ventricle plus septum) (Data not shown). In the lung tissues from MCT-PAH rats, P-PKM2 expression significantly increased compared with the healthy rats, but the total PKM2 expression had no changes (Fig.1B). Additionally, in the isolated RPASMCs, hypoxia ($1\%O_2$) also induced increase of P-PKM2 (Fig.1C). Phosphorylation of PKM2 at Tyr105 remains a major observation known for reduction in PKM2 activity, playing an important role in the pooling of metabolites [22]. Consistently, the decrease in PKM2 activity corresponding with the increased phosphorylation of PKM2 was observed in the serum of MCT-treated rat and the cell lysates generated from hypoxia RPASMCs (Fig.1D&E).

3.3 PKM2 activators could reverse the development of pulmonary hypertension induced by MCT *in vivo*.

To assess definitively the function of PKM2 in regulating the development of PAH, PKM2 activators (L-serine and FBP) were used in the MCT-PAH rats. They were intragastric administration one week after rats developing PAH. L-serine and FBP both could rescue the weight of MCT-induced rats (Fig.2A) and the index of right ventricular hypertrophy (Fig.2B). Lymphoid follicles were induced in the lung on infection or chronic inflammation lymphoid follicles in chronic lung diseases [23] and FBP could attenuate the number of lymphoid follicles, while L-serine had no obvious effects (Fig.2C). Additionally, FBP and L-serine both contributed to the beneficial effects in attenuating pulmonary vascular remodeling in the PAH, including the widened alveolar interval and the decreased wall thickness of small arteries (Fig.2D).

3.4 Increased intracellular ROS generation in PAH.

DCFH-DA was used to test the intracellular ROS generation. RPASMCs treated in hypoxia or isolated from MCT-induced rats both had increased intracellular ROS levels (Fig.3A). The antioxidant NAC, NOX inhibitor apocynin and SOD mimetics MnTBAP which could abolish the intracellular ROS, inhibited the over-proliferation induced by hypoxia (Fig.3B). NAC, apocynin and MnTBAP also could decrease the phosphorylation of PKM2 (Fig.3C) and activated the pyruvate kinase activity (Fig.3D) induced by hypoxia. Concurrently, the lactate production increased in hypoxia by treatment with ROS inhibitors (Fig.3E). As expected *in vivo* PAH rats,

6

NAC could decrease the expression of P-PKM2 in the lung tissues of MCT-induced rats (Fig.3F) and attenuate MCT-induced the development of pulmonary hypertension and vascular remodeling. For example, NAC could reverse the rat weight (Fig.3G), the RV/(LV+S) (Fig.3H), number of lymph follicles (Fig.3I) and wall thickness (Fig.3J) in the MCT-PAH.

3.5 Decreased glycolysis and serine synthesis, increased pentose phosphate pathway in the pulmonary hypertension.

To determine the mechanism that decreased PKM2 activity could promote the development of PAH, we tested the glucose consumption and lactate production in the supernatant of RPASMCs and the MCT-induced rat serum. The glucose consumption had no changes (Fig.4A), but the lactate production significantly decreased (Fig.4B). As a response to oxidative stress, we expected changes in the regulation of the antioxidative capacity of the cells. The mRNA of the antioxidative enzyme catalase and glutathione peroxidase 1 (GPX1) decreased in the RPASMCs in hypoxia for 2h and increased for 24h (Fig.4C). Consistent with the mRNA expression of GPX1, the ratio of GSH/GSSG decreased in the RPASMCs in hypoxia for 2h and increased for 24h (Fig.4D) which means that pentose phosphate pathway may function in this process. Furthermore, there are three enzymes, 3-phospho-glycerate dehydrogenase (PHGDH), phosphoserine aminotransferase 1 (PSAT1), and phosphoserine phosphatase (PSPH), which are required for the three-step conversion of the glycolytic intermediate 3-PG to serine [16]. In the lung tissues from MCT and hypoxia-induced RPASMCs, mRNA expression of PHGDH, PSAT1 and PSPH all decreased (Fig.4E), suggesting the decrease of serine synthesis in the PAH. This implicated that decreased PKM2 activity may favour biomass generation.

3.6 Cav1.2 expression increased in the PAH and it was in the downstream of ROS and PKM2.

Elevation of Ca^{2+} influx in PASMCs plays an important role in PAH. The microRNA-328 regulates hypoxic pulmonary hypertension by targeting at insulin growth factor 1 receptor and L-type calcium channel-alpha1C [24]. We found that under the stimulation of MCT-treatment as well as hypoxia exposure, Cav1.2 protein expression significantly increased in the lung tissues (Fig.5A &B). PKM2 activator and ROS inhibitors could reverse the increased expression of Cav1.2 induced by hypoxia in RPASMCs (Fig.5C&E). Moreover, calcium flux in RPASMCs could be inhibited when adding PKM2 activator and ROS inhibitors (Fig.5D&F). Taken together, Cav1.2 was thus in the downstream of ROS and PKM2.

4. Discussion

In the present study, we have demonstrated that intracellular oxidative stress increased in the RPASMCs from MCT and hypoxia-induced PAH rats. Increasing ROS led to the increased phosphorylation of PKM2 and decreased PKM2 activity. The emerging PKM2 inactivation triggered increased proliferation due to elevated pentose phosphate pathway, decreased glycolysis and serine synthesis. Furthermore, the inactivation of PKM2 also increased the expression of Cav1.2, which also could enhance the proliferation of RPASMCs and promote the hypoxia-induced vasoconstriction.

Previous studies have confirmed increased oxidative stress in the RPASMCs in the PAH. Mitochondria and Nox are the master sources of altered ROS generation in PAH [25]. NADPH

oxidases recently have been proposed as possible pulmonary oxygen sensors for the acute response to hypoxic pulmonary vasoconstriction [26]. Reactive oxygen species (ROS) thus plays a major role in the vascular remodeling that occurs during chronic alveolar hypoxia [27]. However, cellular signaling mechanisms regulated by ROS are still unknown. In respect with the possible mechanism, we found that the isolated RPASMCs were sensitive to 2-DG, an inhibitor of glycolysis, suggesting the glycolysis may function in the development of PAH. Additionally, increased phosphorylation of PKM2 and decreased PKM2 activity in the PAH implicated that PKM2 is a key enzyme, which has been studied in various cancer cells [28]. Then we established MCT-PAH rat models and fed with PKM2 activators L-serine and FBP. Serine is an allosteric activator of PKM2, promoting the shift of the less active dimeric form to an active tetrameric form [29]. Fructose-1,6-bisphosphate (FBP) is an endogenous activator of PKM2 [30]. Surprisingly, they both reversed the development of MCT-PAH.

To determine whether PKM2 was triggered by ROS in vivo, we treated MCT-PAH rats with the antioxidant NAC. This difference in rat weight, RV/(LV+S), number of lymph follicles and wall thickness were alleviated when treated with NAC. This phenomenon shed the light on the benefit of reduced PKM activity is for RPASMCs in PAH. In cancer cells, it has been well-known that lower activity of PKM2 promotes the accumulation of upstream glycolytic intermediates, which are precursors for biosynthesis of nucleotides, amino acids, and lipids required for proliferation [31]. In addition, reduced pyruvate kinase activity in PKM2-expressing cells would lead to accumulation of 3-PG, which could then be converted to serine [16]. The accumulation of glucose-6-phosphate shifts glucose flux through the pentose phosphate pathway (PPP) [18], resulting in decreased lactate production and serine synthesis in the PAH. However, pentose phosphate pathway was appropriately enhanced in order to sustain proliferation through the accumulation of GSH.

Our results also identified Cav1.2 as a potential downstream target of PKM2. Many studies indicated that Cav1.2 is an essential regulator of PA construction [32]. In this study, we found that Cav1.2 expression increased in the PAH and it could be reversed in the treatment with NAC and L-serine.

In this paper, the right ventricular systolic pressure (RVSP) measurement and the metabolic analysis using analysis of ^{13}C-labeled metabolites were lacking because of the limitation of instruments.

In conclusion, our data provide new evidence that PKM2 plays a dominant role in the pathogensis of PAH. Decreased pyruvate kinase M2 confers additional advantages to RPASMCs by allowing them to sustain anti-oxidant responses and thereby support cell survival in PAH. It may become a novel treatment strategy in PAH by using of PKM2 activators.

Conflicts of interest
None.

Glossary

PAH: Pulmonary arterial hypertension
PKM2: pyruvate kinase M2
PASMC: pulmonary artery smooth muscle cells
ROS: reactive oxygen species
MCT: Monocrotaline
GPX1: glutathione peroxidase 1

References

[1] Ioannou CV, Kontopodis N, Metaxa E, Papaharilaou Y, Georgakarakos E, Kafetzakis A, et al. Graft inflow stenosis induced by the inflatable ring fixation mechanism of the ovation stent-graft system: hemodynamic and clinical implications. J Endovasc Ther. 2014;21:829-38.

[2] Liu Y, Ma C, Zhang Q, Yu L, Ma J, Zhang L, et al. The key role of transforming growth factor-beta receptor I and 15-lipoxygenase in hypoxia-induced proliferation of pulmonary artery smooth muscle cells. The international journal of biochemistry & cell biology. 2012;44:1184-202.

[3] Liu XR, Liu Q, Chen GY, Hu Y, Sham JS, Lin MJ. Down-regulation of TRPM8 in pulmonary arteries of pulmonary hypertensive rats. Cellular physiology and biochemistry : international journal of experimental cellular physiology, biochemistry, and pharmacology. 2013;31:892-904.

[4] Sanders KA, Hoidal JR. The NOX on pulmonary hypertension. Circulation research. 2007;101:224-6.

[5] Touyz RM. Reactive oxygen species, vascular oxidative stress, and redox signaling in hypertension: what is the clinical significance? Hypertension. 2004;44:248-52.

[6] Rhoades RA, Packer CS, Roepke DA, Jin N, Meiss RA. Reactive oxygen species alter contractile properties of pulmonary arterial smooth muscle. Canadian journal of physiology and pharmacology. 1990;68:1581-9.

[7] Wolin MS, Ahmad M, Gupte SA. Oxidant and redox signaling in vascular oxygen sensing mechanisms: basic concepts, current controversies, and potential importance of cytosolic NADPH. American journal of physiology Lung cellular and molecular physiology. 2005;289:L159-73.

[8] Frazziano G, Al Ghouleh I, Baust J, Shiva S, Champion HC, Pagano PJ. Nox-derived ROS are acutely activated in pressure overload pulmonary hypertension: indications for a seminal role for mitochondrial Nox4. American journal of physiology Heart and circulatory physiology. 2014;306:H197-205.

[9] Sturrock A, Huecksteadt TP, Norman K, Sanders K, Murphy TM, Chitano P, et al. Nox4 mediates TGF-beta1-induced retinoblastoma protein phosphorylation, proliferation, and hypertrophy in human airway smooth muscle cells. American journal of physiology Lung cellular and molecular physiology. 2007;292:L1543-55.

[10] Veit F, Pak O, Egemnazarov B, Roth M, Kosanovic D, Seimetz M, et al. Function of NADPH oxidase 1 in pulmonary arterial smooth muscle cells after monocrotaline-induced pulmonary vascular remodeling. Antioxidants & redox signaling. 2013;19:2213-31.

[11] Israelsen WJ, Dayton TL, Davidson SM, Fiske BP, Hosios AM, Bellinger G, et al. PKM2 isoform-specific deletion reveals a differential requirement for pyruvate kinase in tumor cells. Cell. 2013;155:397-409.

[12] Li J, Yang Z, Zou Q, Yuan Y, Li J, Liang L, et al. PKM2 and ACVR 1C are prognostic markers for poor prognosis of gallbladder cancer. Clinical & translational oncology : official publication of the Federation of Spanish Oncology Societies and of the National Cancer Institute of Mexico. 2014;16:200-7.

[13] Wong N, De Melo J, Tang D. PKM2, a Central Point of Regulation in Cancer Metabolism. International journal of cell biology. 2013;2013:242513.

[14] Chaneton B, Gottlieb E. Rocking cell metabolism: revised functions of the key glycolytic regulator PKM2 in cancer. Trends in biochemical sciences. 2012;37:309-16.

[15] Luo W, Hu H, Chang R, Zhong J, Knabel M, O'Meally R, et al. Pyruvate kinase M2 is a PHD3-stimulated coactivator for hypoxia-inducible factor 1. Cell. 2011;145:732-44.

[16] Ye J, Mancuso A, Tong X, Ward PS, Fan J, Rabinowitz JD, et al. Pyruvate kinase M2 promotes de novo serine synthesis to sustain mTORC1 activity and cell proliferation. Proceedings of the National Academy of Sciences of the United States of America. 2012;109:6904-9.

[17] Yang W, Xia Y, Ji H, Zheng Y, Liang J, Huang W, et al. Nuclear PKM2 regulates beta-catenin transactivation upon EGFR activation. Nature. 2011;480:118-22.

[18] Anastasiou D, Poulogiannis G, Asara JM, Boxer MB, Jiang JK, Shen M, et al. Inhibition of pyruvate kinase M2 by reactive oxygen species contributes to cellular antioxidant responses. Science. 2011;334:1278-83.

[19] Li S, Ran Y, Zhang D, Chen J, Li S, Zhu D. MicroRNA-138 plays a role in hypoxic pulmonary vascular remodelling by targeting Mst1. The Biochemical journal. 2013;452:281-91.

[20] Morgan HP, O'Reilly FJ, Wear MA, O'Neill JR, Fothergill-Gilmore LA, Hupp T, et al. M2 pyruvate kinase provides a mechanism for nutrient sensing and regulation of cell proliferation. Proceedings of the National Academy of Sciences of the United States of America. 2013;110:5881-6.

[21] Humbert M, Morrell NW, Archer SL, Stenmark KR, MacLean MR, Lang IM, et al. Cellular and molecular pathobiology of pulmonary arterial hypertension. Journal of the American College of Cardiology. 2004;43:13S-24S.

[22] Lv L, Xu YP, Zhao D, Li FL, Wang W, Sasaki N, et al. Mitogenic and oncogenic stimulation of K433 acetylation promotes PKM2 protein kinase activity and nuclear localization. Molecular cell. 2013;52:340-52.

[23] Yadava K, Marsland BJ. Lymphoid follicles in chronic lung diseases. Thorax. 2013;68:597-8.

[24] Guo L, Qiu Z, Wei L, Yu X, Gao X, Jiang S, et al. The microRNA-328 regulates hypoxic pulmonary hypertension by targeting at insulin growth factor 1 receptor and L-type calcium channel-alpha1C. Hypertension. 2012;59:1006-13.

[25] Weissmann N, Zeller S, Schafer RU, Turowski C, Ay M, Quanz K, et al. Impact of mitochondria and NADPH oxidases on acute and sustained hypoxic pulmonary vasoconstriction. American journal of respiratory cell and molecular biology. 2006;34:505-13.

[26] Weissmann N, Sommer N, Schermuly RT, Ghofrani HA, Seeger W, Grimminger F. Oxygen sensors in hypoxic pulmonary vasoconstriction. Cardiovascular research. 2006;71:620-9.

[27] Mittal M, Roth M, Konig P, Hofmann S, Dony E, Goyal P, et al. Hypoxia-dependent regulation of nonphagocytic NADPH oxidase subunit NOX4 in the pulmonary vasculature. Circulation research. 2007;101:258-67.

[28] Chu B, Wang J, Wang Y, Yang G. Knockdown of PKM2 induces apoptosis and autophagy in human A549 alveolar adenocarcinoma cells. Molecular medicine reports. 2015;12:4358-63.

[29] Chaneton B, Hillmann P, Zheng L, Martin AC, Maddocks OD, Chokkathukalam A, et al. Serine is a natural ligand and allosteric activator of pyruvate kinase M2. Nature. 2012;491:458-62.

[30] Anastasiou D, Yu Y, Israelsen WJ, Jiang JK, Boxer MB, Hong BS, et al. Pyruvate kinase M2 activators promote tetramer formation and suppress tumorigenesis. Nature chemical biology. 2012;8:839-47.

[31] Eigenbrodt E, Reinacher M, Scheefers-Borchel U, Scheefers H, Friis R. Double role for pyruvate kinase type M2 in the expansion of phosphometabolite pools found in tumor cells. Critical reviews in oncogenesis. 1992;3:91-115.

[32] Hirenallur SD, Haworth ST, Leming JT, Chang J, Hernandez G, Gordon JB, et al. Upregulation of vascular calcium channels in neonatal piglets with hypoxia-induced pulmonary hypertension. American journal of physiology Lung cellular and molecular physiology. 2008;295:L915-24.

Figure legends

Figure 1. Increasing expression of P-PKM2 in the lung tissues from pulmonary hypertension rats.

A. Effects of different concentration of 2-DG (n=8) and oligomycin (n=8; P=NS) on the intracellular ATP production in the cultured RPASMCs. 2-DG is an inhibitor of glycolysis and oligomycin is the inhibitor of oxidative phosphorylation.

B. Western blot analysis of P-PKM2 and PKM2 expression in the lung tissues from MCT-induced PAH rats. Quantitative analysis was presented in the graph. Data were normalized to β-actin (n=5).

C. Western blot analysis of P-PKM2 and PKM2 expression in RPASMCs treated in normoxia and hypoxia. Quantitative analysis was presented in the graph. Data were normalized to β-actin (n=3).

D. Pyruvate kinase catalytic activity in the serum from the MCT rats and the healthy rats (n=5).

E. Pyruvate kinase catalytic activity from normoxia and hypoxia-treated RPASMCs (n=5). Results represented mean ± SEM of n independent experiments. NS, not significant. **$P<0.01$, *$P<0.05$, 1-way ANOVA.

Figure 2. PKM2 activators attenuated MCT-induced the development of pulmonary hypertension and vascular remodeling.

A. Rat weight was evaluated when treated with PKM2 activators, L-serine (315mg/kg) and FBP (460mg/kg) in MCT-induced PAH (n=6).

B. Fulton index: RV/(LV+S). The right ventricle (RV) to left ventricle (LV) plus septum (S) ratio was quantified when treated with PKM2 activators, L-serine and FBP in MCT-induced PAH (n=6).

C. Left: Representative micrographs of lymphoid follicles (LFs) located between pulmonary arteries and stained by hematoxylin and eosin; right: Lymphoid follicles were counted on the per entire lung slide when treated with L-serine and FBP in MCT-induced PAH (n=6). Scale bars, 100um.

D. Representative micrographs of pulmonary alveoli and the PA wall thickness on lung sections when treated with L-serine and FBP in MCT-induced PAH (n=6). Scale bars, 50um. Results represented mean ± SEM of n independent experiments. **$P<0.01$, *$P<0.05$, 1-way ANOVA.

Figure 3. Increased intracellular ROS generation in PAH.

A. ROS staining was performed using DCFH-DA in RPASMCs treated in hypoxia or isolated from MCT-induced PAH rats. Left: Representative images of ROS staining; right: Statistics of ROS

fluorescence intensity in per picture (n=8). Scale bars, 100um.

B. Effects of antioxidants (NAC, apocynin and MnTBAP) on the over-proliferation of RPASMCs induced by hypoxia in vitro (n=10).

C. Western blots analyzed the effects of ROS inhibitors on the expression of P-PKM2 in RPASMCs in hypoxia (n=3). Nor, normoxia; apoc, apocynin; Mn, MnTBAP.

D. Pyruvate kinase catalytic activity from hypoxia-treated RPASMCs with the treatment of different ROS inhibitors (n=5).

E. Effects of ROS inhibitors on the lactate production in the supernatant of RPASMCs (n=4).

F. Effects of NAC on the expression of P-PKM2 and PKM2 in the lung tissues of the MCT-induced PAH rats (n=5).

G. Rat weight was evaluated in rats when treated with the antioxidant NAC in MCT-induced PAH rats (n=5).

H. RV/(LV+S) was calculated in rats when treated with the antioxidant NAC in MCT-induced PAH rats (n=5).

I. Effects of NAC on the number of lymph follicles in the lung tissues of MCT-induced PAH rats (n=5).

J. Effects of NAC on the pulmonary alveoli and the PA wall thickness in MCT-induced PAH rats. Quantitative analysis is presented in the graph. Scale bars, 50um. Results represented mean ± SEM of n independent experiments. **$P<0.01$, *$P<0.05$,1-way ANOVA.

Figure 4. Decreased glycolysis and serine synthesis, increased pentose phosphate pathway in the pulmonary hypertension.

A. The glucose consumption had no change in the supernatant of RPASMCs in hypoxia (n=3,P=NS) and in the MCT rat serum (n=5,P=NS) compared to controls.

B. The production of lactate decreased in the supernatant of RPASMCs in hypoxia (n=4) and in the MCT rat serum (n=5) compared to controls.

C. Quantitative PCR results. The mRNA expression of anti-oxidative enzyme GPX1 in the RPASMCs in hypoxia for 2 hours and 24 hours (n=3).

D. The ratio of GSH/GSSG in the RPASMCs treated in hypoxia for 2 hours and 24 hours (n=3).

E. The mRNA expression of key enzymes involved in serine synthesis, including PHGDH, PSAT1 and PSPH from the lung tissues of MCT (n=5) and RPASMCs in hypoxia compared to control (n=4). Results represented mean ± SEM of n independent experiments. NS, not significant. **$P<0.01$, *$P<0.05$,1-way ANOVA.

Figure 5. Cav1.2 expression increased in the PAH and was inhibited by ROS inhibitors and PKM2 activators.

A. Western blot analysis of Cav1.2 expression in the lung tissues from MCT-induced PAH rats. Quantitative analysis was presented in the graph. Data were normalized to β-actin (n=4).

B. Western blot analysis of Cav1.2 expression in the lung tissues from hypoxia-induced PAH rats. Quantitative analysis was presented in the graph. Data were normalized to β-actin (n=6).

C. Effects of L-serine on the expression of Cav1.2 in RPASMCs treated in hypoxia. Data were normalized to β-actin (n=3).

D. Effects of PKM2 activators (L-serine and FBP) on intracellular calcium concentration in RPASMCs. RPASMCs were loaded with Furo-8 for 30 minutes, as described in 'Materials and Methods'. Baseline $[Ca^{2+}]_i$ was recorded, followed by sequential additions of 80 mM KCl at the 150th picture (n=10).

E. Effects of ROS inhibitors (NAC, apocynin and MnTBAP) on the expression of Cav1.2 in RPASMCs treated in hypoxia. Nor, normoxia; Apop, apocynin; Mn, MnTBAP. Data were normalized to β-actin (n=3).

F. Effects of ROS inhibitors (NAC, apocynin and MnTBAP) on intracellular calcium concentration in RPASMCs. Baseline $[Ca^{2+}]_i$ was recorded, followed by sequential additions of 80 mM KCl at the 150th picture (n=10). Results represented mean $\pm$ SEM of n independent experiments. *$P<0.05$,1-way ANOVA.
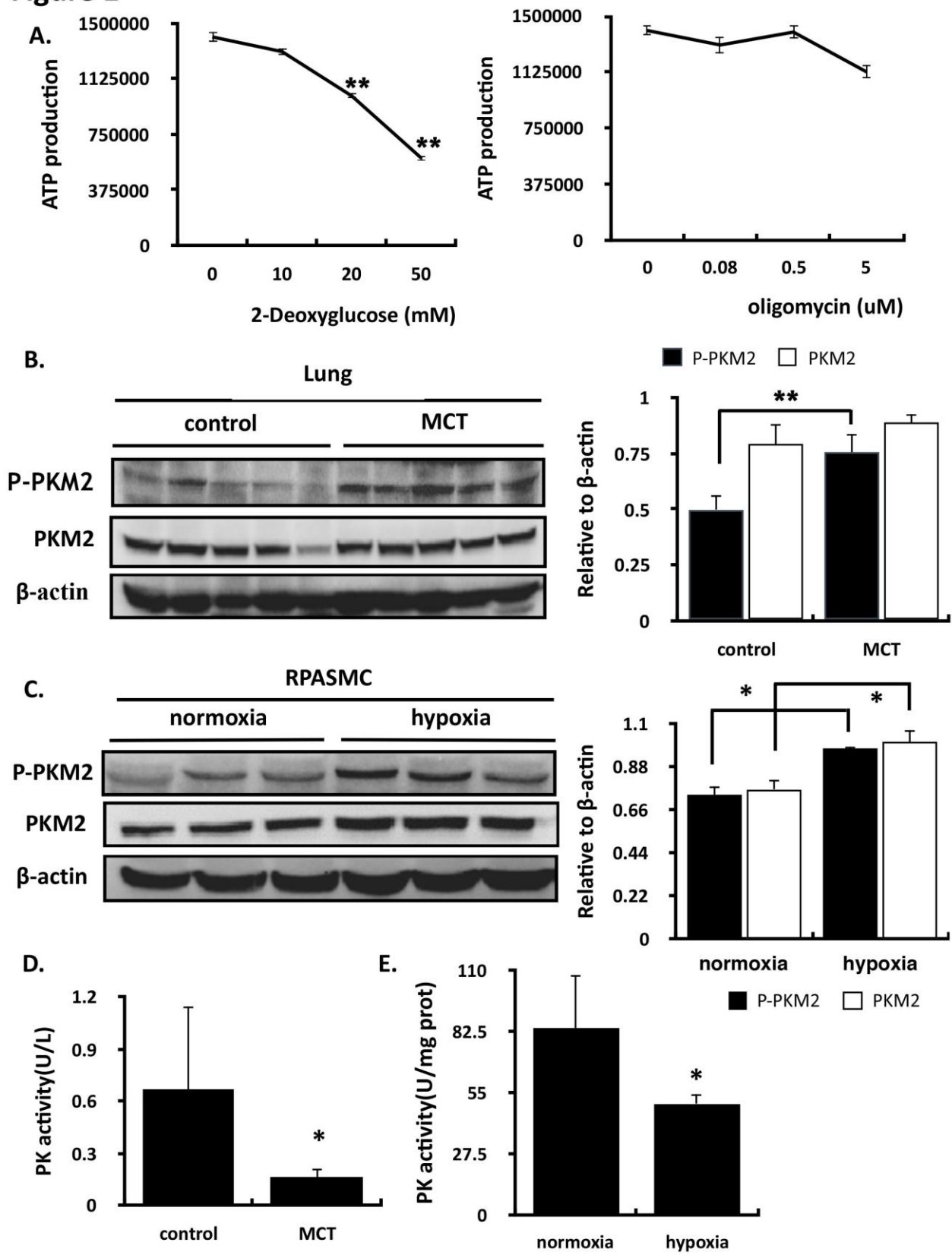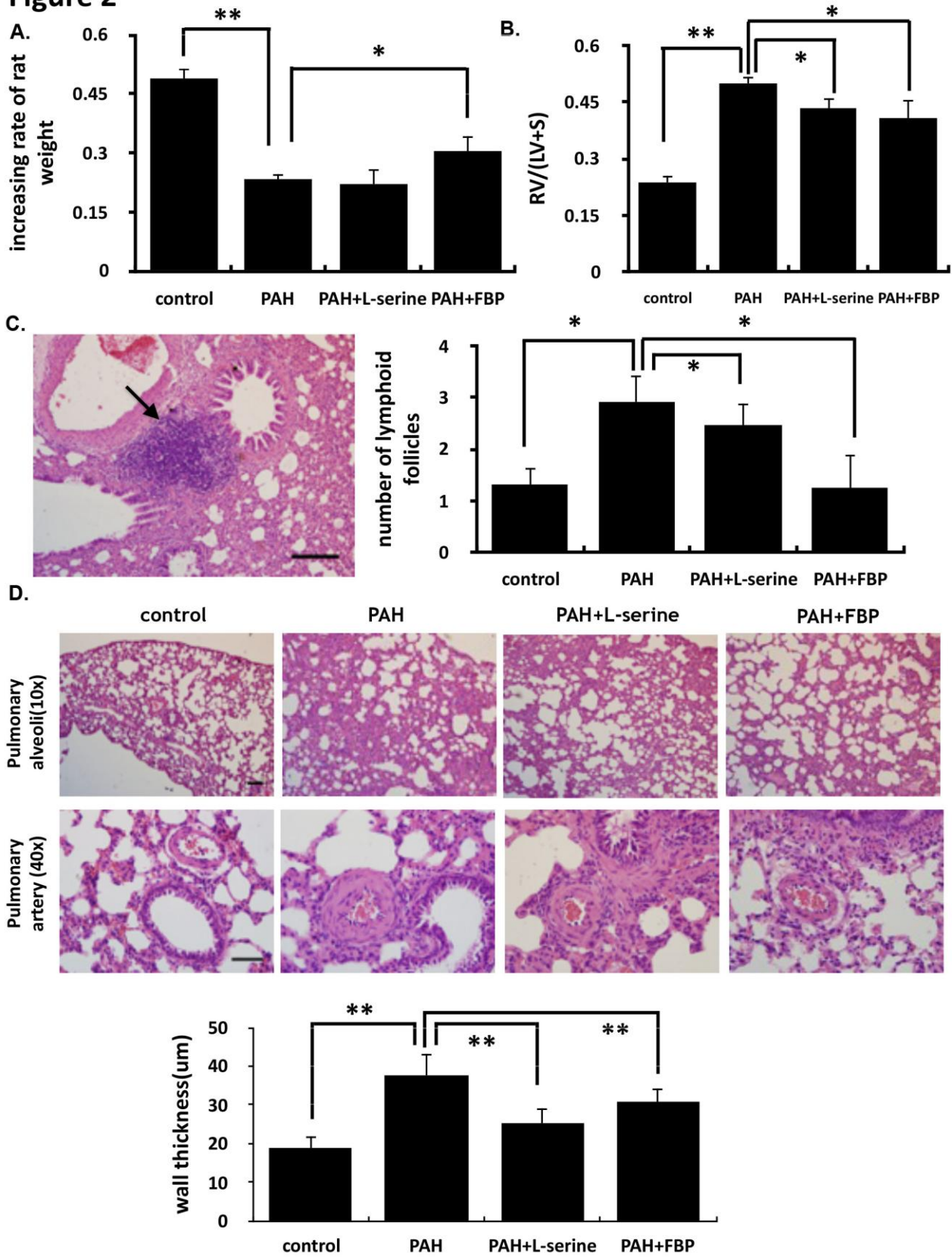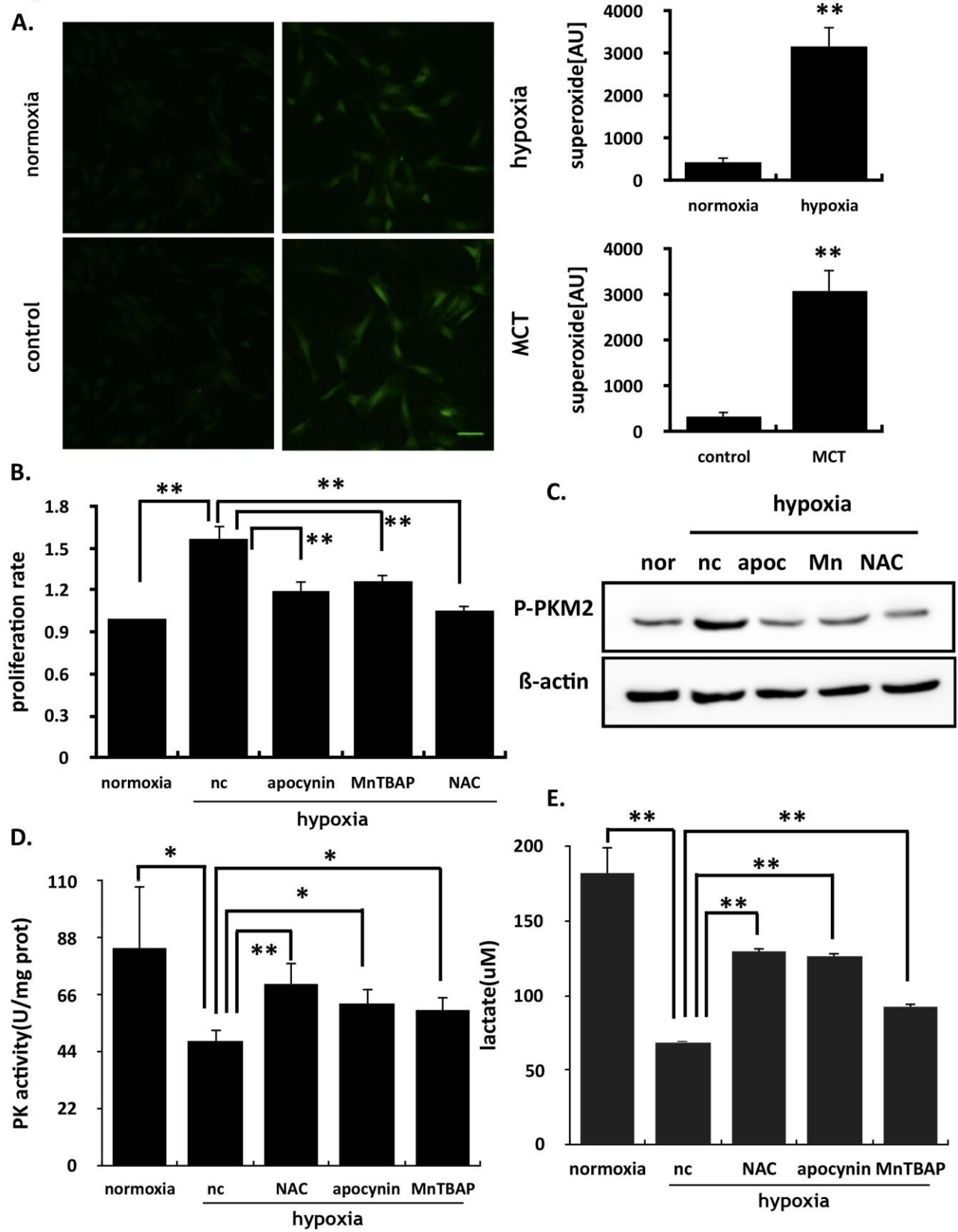
13

Figure 1

Figure 2

Figure 3

A.

B.

C.

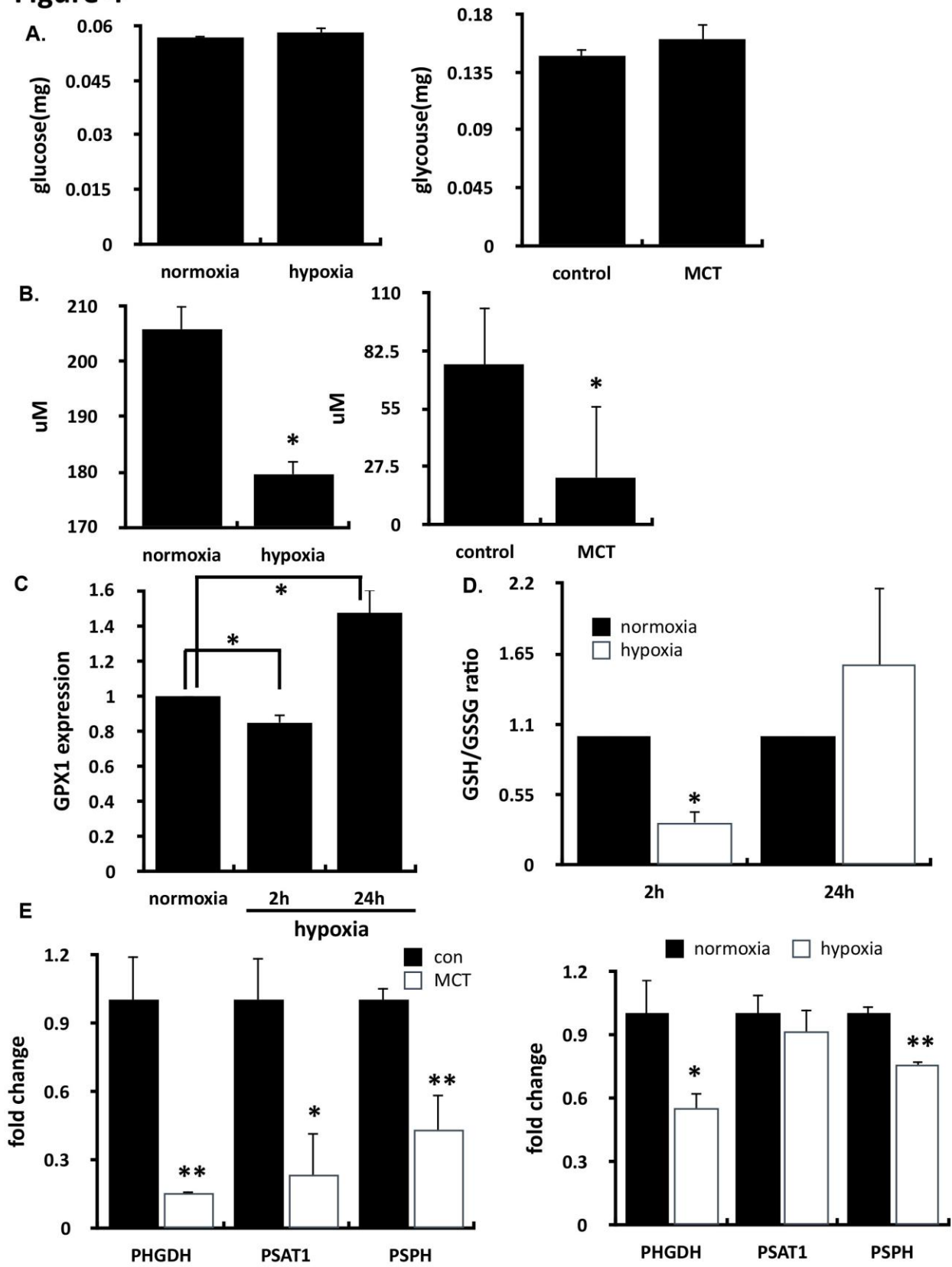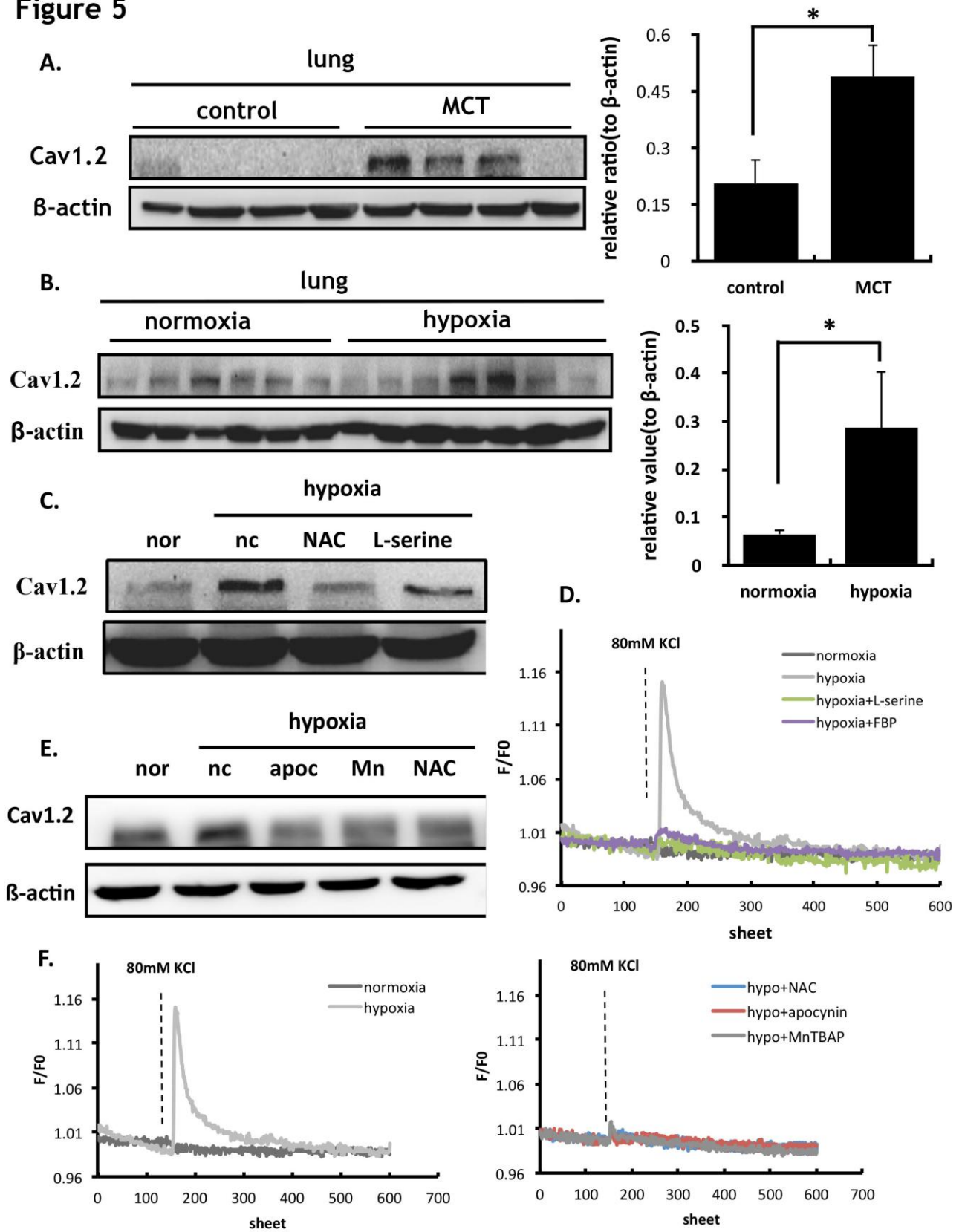
D.

E.
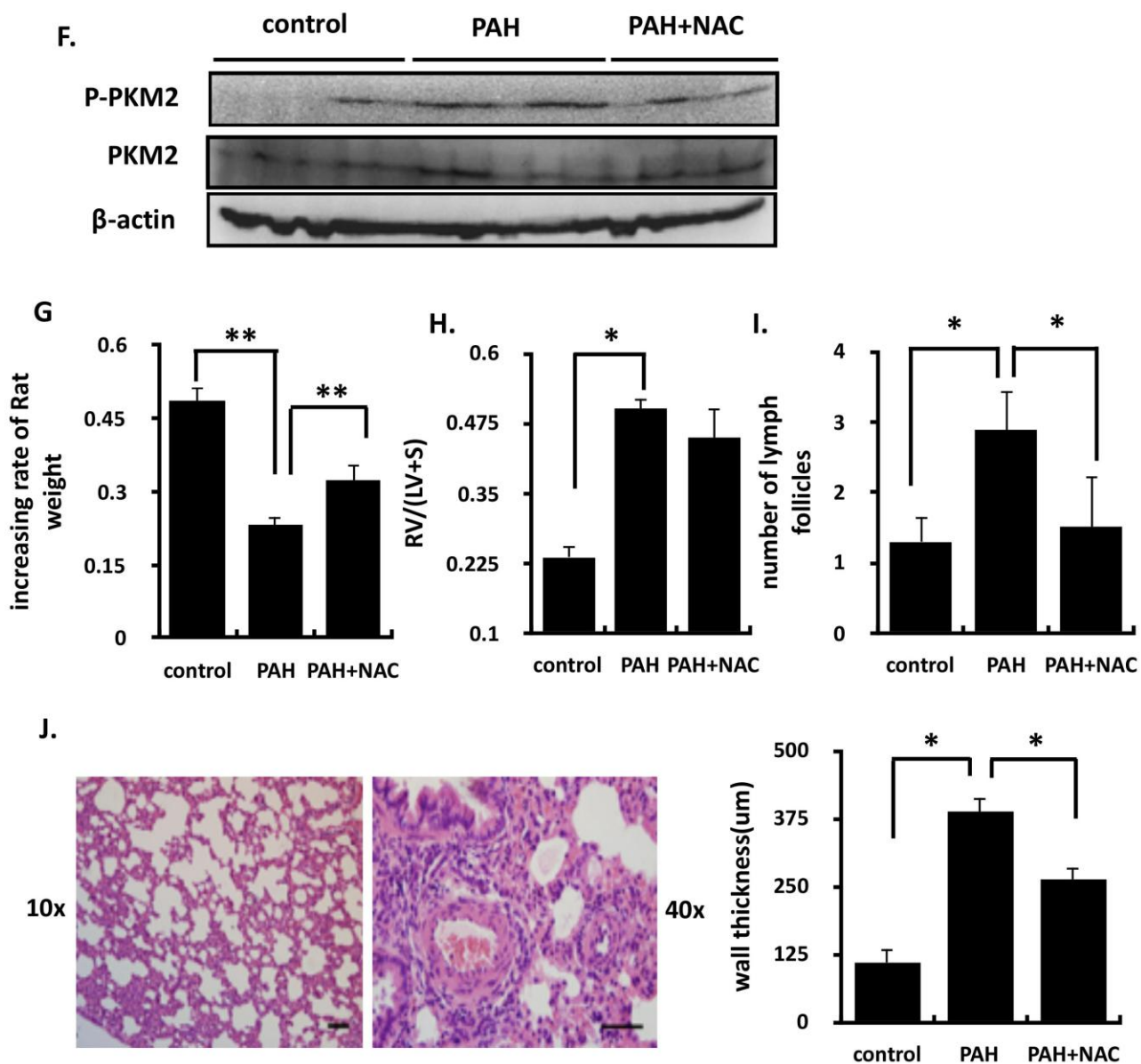
Figure 3

Figure 4

Figure 5

Highlights:

- Decreased pyruvate kinase M2 activity confers to the development of PAH.
- ROS-PKM2-Cav1.2 axis functions in the PAH.
- PKM2 activators may become a novel treatment strategy in PAH.